Mon. Not. R. astr. Soc. (1989) **241**, 559–573

Light curve analysis and parameter study of the EB-type eclipsing binary V 836 Cygni

Robert A. Breinhorst, Josef Kallrath and Bernd-Christoph Kämper *Astronomische Institute der Universität Bonn, Auf dem Hügel 71, 5300 Bonn 1, FRG*

Accepted 1989 May 10. Received 1989 April 24; in original form 1989 January 24

Summary. The EB-type short-period eclipsing binary V 836 Cygni has been analysed on the basis of earlier published and hitherto unexploited fairly extensive *UBV* photometry. The Simplex method for parameter optimization, applied to the Wilson–Devinney model approach, proved a very effective tool to determine the best-fit solution. The corresponding global minimum of σ_{fit}, however, is only marginally pronounced, and thereby allows the light curve to be fitted over a whole range of parameters (with a mass-ratio interval $0.3 \leq q \leq 0.5$). This indeterminacy, likely to result from the low secondary light level relative to the observational noise, probably explains the discrepancies of previous photometric and spectroscopic analyses. It is partly overcome by evaluating the four-colour Strömgren observations contained in the photometric binary-star survey of Hilditch & Hill, which determine, through comparison with the calibrated synthetic photometric grids of Lester, Gray & Kurucz and in combination with the mass function, a fairly accurate parameter set and indicate a low mass ratio near $q \approx 0.34$. The system thus appears to have evolved already through the stage of rapid mass exchange with mass-ratio reversal, as the primary component is an almost normal A0 V star, whilst the G-type secondary, oversized and therefore overluminous compared to a main-sequence star of its surface brightness, is in marginal contact with its Roche lobe.

1 Introduction

The EB-type eclipsing binary V 836 Cygni (BD + 35° 4496 = HD 203470, A0, $P = 0.653$ d) has been subject to several observational studies over recent years (Wester 1977; Duerbeck & Schumann 1982; Breinhorst & Duerbeck 1982, hereafter referred to as Paper I). While their basic results, pointing towards an unevolved main-sequence system with a primary component A0 V (MK classification according to Hill *et al.* 1975) almost filling up its Roche limiting surface, seem to be in qualitative agreement, quantitative inconsistencies between several of the system parameters remain to be explained.

Wester's photometric analysis of his B and V light-curve observations, based on the Hutchings & Hill (1971) light-curve synthesis program, and alternatively on the model of Wood (1971), yields a mass ratio q of the order of 0.5. It has been noted already (Paper I), that under the assumption of two main-sequence components (the primary's mass being estimated from its A0 V spectral type) both the spectroscopic mass function (Duerbeck & Schumann 1982) and the surface intensity ratio (as obtained from the light curve solutions) indicate a lower value of q, confined somewhere between $0.30 < q < 0.38$.

Though this inequality appears to confirm a general trend, commonly ascribed to unreconciled errors in the reduction of binary spectra, the discrepancy here may partly be attributed to the underlying photometric data. Wester already notes himself that his observations, considerably contaminated by unfavourable sky conditions, and, moreover, partly influenced by internal light-curve fluctuations, may be insufficient to yield a precise solution even within the frame of Roche geometry. The indeterminacy of Wester's system parameters, resulting from a high noise level, is illustrated by the ambiguity of his Wood-model solution, where the final parameters strongly depend on the input parameter set. The problem may be further aggravated through an inadequate model approximation of the presumably highly distorted stellar figures by the classical Russell–Merrill (1952) method, as can be seen from a variety of earlier discordant results given by previous authors (*cf.* Paper I).

The Wilson–Devinney (1971) model, version 1978, combined with the SIMPLEX optimization algorithm (as introduced and described by Kallrath & Linnell 1987 for light curve analysis) has therefore been used to re-analyse the light curve on the basis of independent observational data. For this purpose three sets of UBV light curves have been presented (*cf.* Paper I, figs 1–3; the individual magnitude differences in the instrumental system have been published in Duerbeck & Breinhorst 1984), each sample collected over relatively short time intervals ($\Delta t < 100P$) independently in 1971 (DB1), 1976 (DB2) and 1980 (BR). This technique is successfully applied (see e.g. Hilditch 1981) to reduce the sometimes enhanced scatter (resulting from transient – i.e. cycle-to-cycle – variations of the light curve) down to the 'normal' observational scale, while superimposed distortions, if actually present, may be seen more clearly.

A comparison of these observations with previously published light curves reveals, apart from a sometimes prominent overall scattering, two distinct features, which in several cases superimpose the normal geometric eclipse curve, and consequently will deteriorate any model solution applied to these observations. There are

(i) a global (i.e. overall) distortion of the light curve, occurring in a few cases, and manifested through a modest asymmetry of the maxima, and

(ii) local distortions, predominantly confined to a phase range around secondary minimum, which are quite prominent in some light curves. The U light curves observed in 1976 and 1980 show this effect, documented by a brightness deficiency on the ascending and descending branches of minimum II, quite clearly.

The present analysis has therefore been restricted primarily to the B and V light curves.

2 Photometric analysis and system parameters

Since the SIMPLEX algorithm implies a gradient-free global optimization technique, in principle no preliminary input parameters need to be determined. We note that the method of differential corrections, when used to search for equal-variance contours in the multi-dimensional parameter space (e.g. by stepping through a discrete set of fixed i, q parameters), may be equally suited (though much less effective) to finding a minimum solution even in a

broad region of shallow variance (Rafert & Markworth 1986). However, in order to avoid severe correlations with secondary parameters, which may easily result in spurious solutions, the number of adjustable parameters should be restricted (when spectroscopic data for the primary component are available, perhaps to the 'conservative' set: inclination i, mass ratio q, temperature T_2, surface potentials Ω_1, Ω_2, and luminosity L_1). An adequate choice of fixed parameters with appropriate values is advisable then.

Therefore, as a starting hypothesis, the system was assumed to consist (in accordance with the MK classification of Hill *et al.* (1975) and the photometric intensity ratio, *cf.* Koch 1973) of two main-sequence components of spectral types A0 and G1, respectively. The list of correspondingly chosen fixed parameters is given in Table 1. In this context the choice for the effective temperature T_1 of the primary, namely the value taken by Wester from Harris (1963) appears to be unduly high. Recent work on the improvement of effective temperature scales (*cf.* Böhm-Vitense 1981), however, seems to allocate $T_{\rm eff}$ around 9700–10 000 K for an A0 V star. But this is the mean effective temperature; the polar temperature referred to in the Wilson–Devinney code then has to be higher (by ≈ 500 K, in this case). With these premises, we decided to fix the polar temperature T_1 at 10 800 K, in order to have a direct intercomparison with the results obtained by Wester (1977) at this temperature with the light curve synthesis program of Hutchings & Hill (1971).

To determine a preliminary solution, the SIMPLEX optimization procedure was first applied to the BR data only. It is immediately realized (Table 2) that most simultaneous B and V solutions, though started with different initial simplices, agree fairly well, while for the individually fitted light curves mutual consistency in B and V is achieved only under identical starting conditions. We note, however, that most solutions, irrespective of colour and type, are of almost identical quality, the respective values for $\sigma_{\rm fit}$ being comparable with the observational scatter (where $\sigma_{\rm obs} = 0.008$ is estimated from the observational noise of comparison star measurements). The resulting fits to the individual B and V light curves yield a satisfactory global light-curve representation (Fig. 1). According to our light curve solutions, secondary eclipse is a grazing total, which is indicated also by the flat-bottomed minimum II in our light curves (*cf.* Paper I). During primary eclipse which is a transit, the fractional light loss from component 1 is approximately 44 per cent.

The subsequent analysis of the complete data set (individual B, V curves of DB1, DB2 and BR and tentatively the U data of DB1 and BR), performed alternatively under application of the differential corrections procedure, gave rise to only slight modifications. It is recognized (Table 3), that all solutions are fairly close to the initial SIMPLEX solutions (B1 being used as

Table 1. Fixed input parameters[1] for the light curve analysis of V 836 Cyg.

Colour	U	B	V
λ (nm)	365	435	550
x_1	0.40	0.47	0.42
x_2	0.84	0.84	0.69
g_1		1.00	
g_2		0.32	
A_1		1.00	
A_2		0.50	
T_1 (K)		10 800	

[1] T_1 = Polar temperature of the primary; x = limb-darkening coefficient; g = gravity darkening exponent; A = bolometric Albedo.

Table 2. Individual B, V and simultaneous $B+V$ light-curve solutions (Wilson–Devinney + SIMPLEX) for data set BR. Solutions from different initial simplices are numbered sequentially.[1]

Solution	B1	V1	BV1	B2*	V2*	BV2	BV3	BV4
i	82.7°	82.5°	82.7°	80.7°	80.0°	82.7°	82.6°	81.6°
q	0.42	0.46	0.43	0.41	0.42	0.43	0.43	0.52
Ω_1	2.92	2.96	2.92	2.86	2.86	2.93	2.93	3.09
Ω_2	2.98	3.17	3.04	2.92	2.91	3.06	3.03	3.38
r_1	0.413	0.417	0.416	0.425	0.426	0.416	0.415	0.404
r_2	0.251	0.247	0.250	0.261	0.268	0.249	0.252	0.247
$k=r_2/r_1$	0.608	0.592	0.601	0.613	0.629	0.599	0.607	0.611
J_2/J_1 (B)	0.049		0.051	0.016		0.051	0.054	0.039
J_2/J_1 (V)		0.082	0.089		0.032	0.089	0.093	0.072
T_2(K)	5474	5425	5516	4633	4551	5517	5564	5274
Iterations	70	75	105	136	68	212	200	89
$\sigma_{fit}[10^{-3}]$	8.4	8.0	8.5	9.2*	9.8*	8.4	8.5	8.5

[1] i = Inclination; $q = \mathcal{M}_2/\mathcal{M}_1$ mass ratio; T_2 = polar temperature of secondary; $r_{1,2}$ = mean (equal volume) radii; $k = r_2/r_1$ ratio of radii; J_2/J_1 = polar flux ratio; $\Omega_{1,2}$ = Roche potentials; σ_{fit} = standard deviation of residuals (in l.u.).
* marks SIMPLEX solutions that did not converge properly (local SSR minima).

Table 3. Independent results of DB1, DB2 and BR light-curve solutions in U, B and V (Wilson–Devinney program with differential corrections optimization).

Data[1]	DB1(U)	DB1(B)	DB1(V)	DB2(B)	DB2(V)	BR(U)	BR(B)	BR(V)
i	82.0°	80.6°	80.5°	81.5°	80.9°	81.6°	82.1°	80.0°
q	0.41	0.39	0.40	0.40	0.39	0.42	0.39	0.41
Ω_1	2.87	2.84	2.82	2.83	2.84	2.89	2.87	2.85
Ω_2	2.88	2.82	2.82	2.88	2.85	2.89	2.86	2.85
r_1	0.422	0.424	0.430	0.428	0.424	0.421	0.418	0.426
r_2	0.265	0.264	0.279	0.259	0.258	0.269	0.257	0.271
$k=r_2/r_1$	0.628	0.623	0.628	0.605	0.609	0.640	0.614	0.635
J_2/J_1	0.053	0.043	0.085	0.018	0.134	0.033	0.060	0.076
T_2(K)	6006	5374	5463	4683	6029	5607	5679	5343

[1] Data sets obtained in 1971(DB1), 1976(DB2) and 1980(BR), see references given in the text. Other symbols as in Table 2.

input parameter set) with only slightly lowered values of q at a modest increase in T_2. Restarting the program, however, with deliberately chosen 'false' input values ($0.20 \leq q \leq 0.50$) brought about considerably deviating solutions, even with an increased number of iterations.

These results, while confirming internal consistency of all light curves obtained in different colours and at different epochs, lead us to suspect an only weakly determined or spurious solution. To explore this possibility of indeterminate parameters, i.e. fits of comparable quality for an extended range of parameter values, the so-called grid method was chosen to solve at fixed equidistant q values ($q = 0.1, 0.2, \ldots 0.8$; one additional point at $q = 0.33$) for the remaining adjustable parameters. The results obtained on the B curve of BR with the SIMPLEX optimization are plotted in Fig. 2 as a function of the photometric mass ratio. Note that the σ_{fit}-curve is almost flat for $q \geq 0.3$ (again bending upwards slowly for $q > 1.0$). This implies that there indeed exists a considerable parameter correlation, i.e. for a wide range of q values the light curve can be fitted at almost equal accuracy ($\sigma_{fit} \approx \sigma_{obs} \approx 0.008$), the variation of q being compensated for by corresponding changes of the other parameters (mainly T_2 and $\Omega_{1,2}$).

The reason for this behaviour is likely to be found in the particular binary configuration encountered here, with a very low contribution L_2 (about three times σ_{obs}) and only a modest deformation of component 1 which appears well detached, independent of the assumed q (*cf.* Fig. 2b). As the secondary minimum is dominated by the gravity-darkening effect of the primary component, the photometric effects are almost the same whether one has small q (and

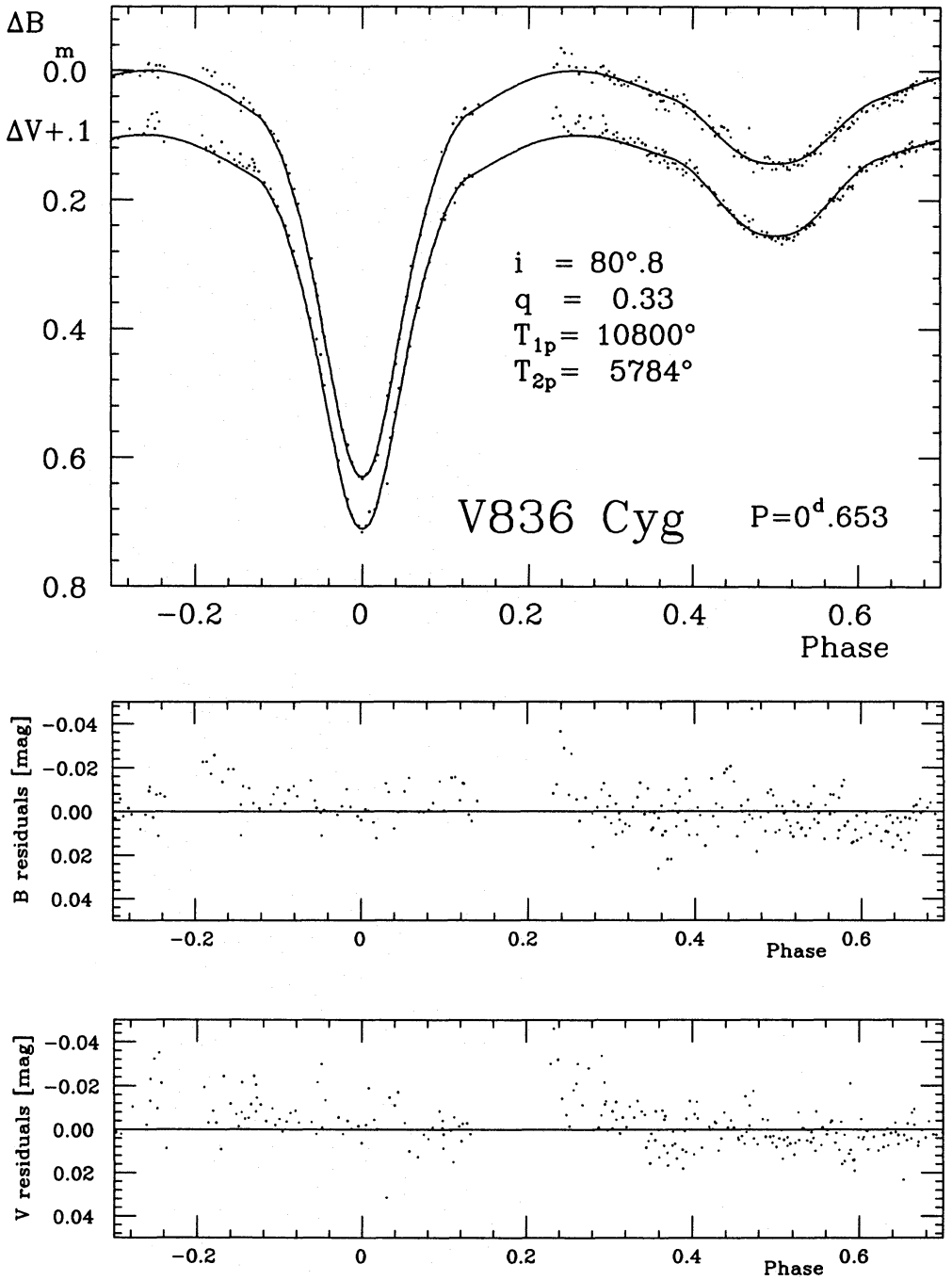

Figure 1. *B* and *V* light curves and residual plots (observations of 1980; data set BR) for a reference solution (Table 4; $q = 0.33$); other fixed parameters as in Table 1.

lower ellipticity of the primary) and somewhat higher L_2, or higher q (increased ellipticity) with a somewhat reduced L_2 (*cf.* also the discussion of a quite similar system, EG Cep, by Kaluzny & Semeniuk 1984). The foregoing analysis therefore readily explains the discrepancies of earlier photometric investigations, but necessarily fails to determine a mass ratio and thereby a definite photometric solution. To constrain the solution more effectively, we either have to make additional assumptions or need external evidence, e.g. from multicolour photometry.

Tentatively, we first imposed a constraint that the solution should be compatible with an assumed 'main-sequence' mass and radius of one component (the appendix describes how this

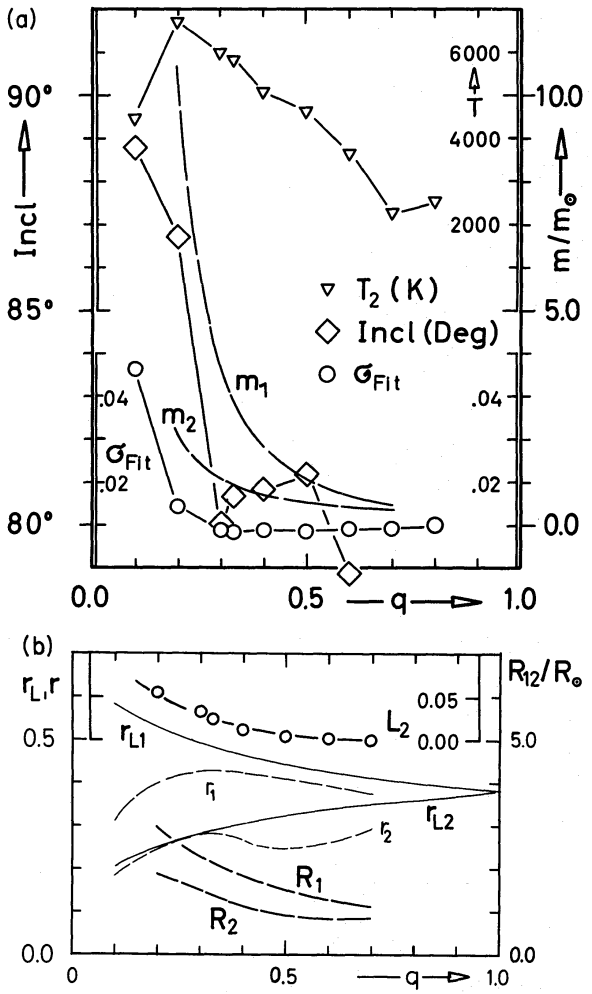

Figure 2. Parameter study for V 836 Cygni: grid solutions for the B curve at fixed equidistant values of q (with an additional point at $q = 0.33$). (a) Dependence upon q of the standard deviation in light units, σ_{fit}, inclination, i, polar temperature of the secondary, T_2, and resulting masses, computed for the mass function $f(\mathcal{M}) = 0.055$ (see text). (b) The same for the relative radii, r, Roche lobe radii, r_{L}, absolute radii, $\mathcal{R}/\mathcal{R}_\odot$ and the fractional luminosity of the secondary, L_2.

constraint may be added to the optimization algorithm). We assumed hypothetically that the secondary component might be a main-sequence star, since the spread in masses and radii for a given spectral class is smaller on the lower main sequence. Furthermore, if the system were prior to the phase of rapid mass exchange (as hitherto assumed), the G Star should be the less evolved of the two components. Under the constraints $\mathcal{M}_2 = 1.0\mathcal{M}_\odot$, $\mathcal{R}_2 = 1.0\mathcal{R}_\odot$ we achieved mass ratios near 0.6 which do not fit at all to the spectroscopic mass function. Obviously the assumption that star 2 might be a main-sequence star is wrong.

3 Radiative properties and atmospheric parameters from Strömgren colours

Though the photometric solution, and in particular the mass ratio, remains indeterminate, additional independent information is available on the radiative properties of the system by evaluating the colour indices and relating them to the atmospheric parameters (T_{eff}, log g and $[M/H]$), thereby providing a comparative test with the photometric results. Unfortunately, none of the necessary pre-requisites (namely the construction of an unreddened, standardized, medium-band colour curve), can be met with the present broad-band UBV data, which are

moreover uncalibrated despite several trials (that remained unsuccessful, however) under only marginal sky conditions. It is nevertheless possible to extract some basic information for the relevant parameters from the Strömgren four-colour observations contained in the photometric survey of northern binary stars by Hilditch & Hill (1975). For V 836 Cyg the catalogue lists colour indices observed at five different phases; the typical standard deviation for catalogue data in the magnitude range $7 < V < 9$, as quoted by the authors, is $\pm 0^{m}.020$, $0^{m}.010$, $0^{m}.010$ in $(u-b)$, $(v-b)$ and $(b-y)$, respectively, or $\pm 0^{m}.022$, $0^{m}.015$ in the calculated c_1, m_1 indices.

Since the quality of our light-curve fits has proven insensitive to the exact value of q chosen, we may adopt any reasonable value for discussing the expected colours and colour changes. In the following, we are referring to a simultaneous B and V SIMPLEX solution at $q = 0.33$ (Table 4) as our reference model solution.

A plot of the Strömgren indices against phase (Fig. 3), in conjunction with synthetic colour curves generated from the reference model solution [and using $uvby$ flux ratios as predicted by the Kurucz (1979) models], immediately shows that the phase-dependent colour variation (when compared with the mean) barely exceeds the observational scatter. Since the Strömgren colour observations were sampled over only a few phases not coinciding with the exact positions of the light-curve extrema, they appear to be almost completely dominated by random variations. Only $(b-y)$ is seen to follow roughly the expected trend (i.e. exhibiting a blue- and red-excess at minima II and I, respectively). With these premises, mean values were

Table 4. Simultaneous $B+V$ reference solution[1] for data set BR, mass ratio fixed at $q = 0.33$.

		Primary	Secondary
i		80.8° ± .4°	
Ω		2.76	2.59
Ω_i		2.53	
f		0.91 ± .01	0.98 ± .02
r_{pole}		0.408	0.256
r_{side}		0.429	0.265
r_{back}		0.444	0.290
r_{point}		0.465	0.315
$\bar{r}$		0.427 ± .005	0.271 ± .010
$k = r_2/r_1$		0.63 ± .02	
T_p	(K)	10800	5784
T_m	(K)	10333	5681
L_2	(B)	0.028 ± .009	
	(V)	0.045	
J_2/J_1	(B)	0.079	
	(V)	0.126	
$\overline{J_2/J_1}$	(B)	0.070 ± .020	
	(V)	0.116	

[1] Ω_i = Critical Roche potential; $f = (\Omega_i - \Omega)/\Omega_i + 1$ fill-out parameter; L_2 = normalized luminosity; $\overline{J_2/J_1}$ = mean surface brightness ratio. T_p, T_m = polar temperature and corresponding flux averaged mean temperature. Quoted errors correspond to a variation of ±0.04 in q.

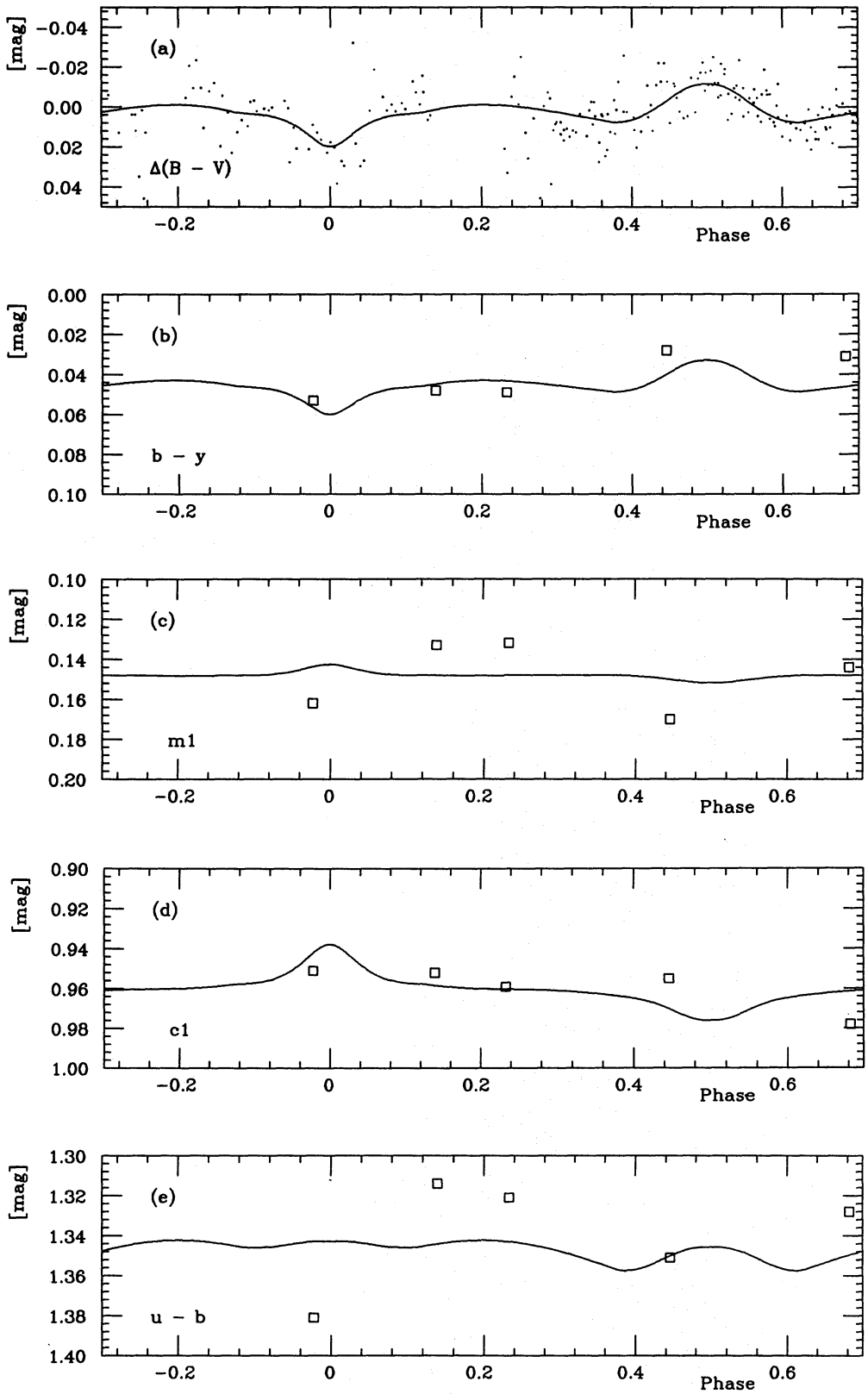

Figure 3. (a) Observed differential $(B-V)$ colours (instrumental system), in the sense 'variable minus comparison', and calculated colour curve (generated from the reference solution at $q=0.33$). (b)–(e) Strömgren indices measured by Hilditch & Hill (1975) and corresponding (reddened) synthetic colour curves (with flux ratios and limb-darkening coefficients predicted from the Kurucz 1979 models and other parameters taken from the reference solution).

formed for the Strömgren indices, yielding

$c_1 = 0.959 \pm 4$, $m_1 = 0.148 \pm 7$, $(b-y) = 0.042 \pm 5$, $(u-b) = 1.339 \pm 11$,

for the combined light of both components. The low-amplitude variation of the colour indices shown in Fig. 3 gives further evidence that the contribution of component 2 is in the range of a few per cent only. It was therefore removed by simply applying differential corrections ($\Delta c_1 = +0.015$, $\Delta m_1 = +0.004$, $\Delta(b-y) = -0.016$, at quadrature), calculated from our reference model solution. These corrections are insensitive to the exact colours adopted for

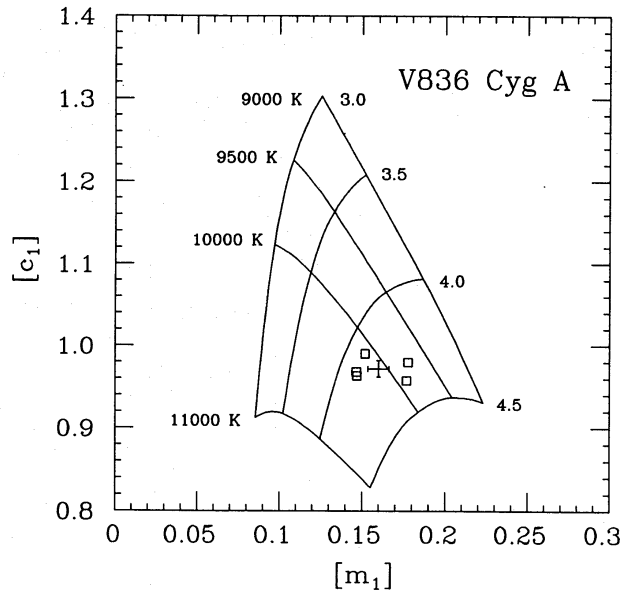

Figure 4. Variation of $[c_1]$ versus $[m_1]$. Measured values at five phases, taken from the survey by Hilditch & Hill (1975) and corrected for the contribution of the secondary are represented by open squares; also shown is the mean value (with error bars). The theoretical log g versus log T_c grid of Lester, Gray & Kurucz (1986) for solar abundances indicates $T_c \approx 10\,080$ K, log $g \approx 4.22$.

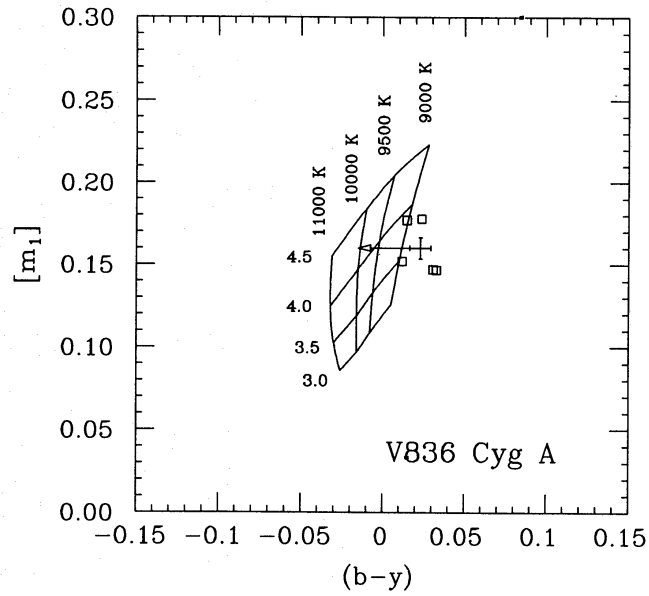

Figure 5. Variation of $[m_1]$ versus $(b-y)$. Consistency with Fig. 4(a) requires a reddening correction of $E(b-y) = 0.038$ and gives $(b-y)_0 = -0.015$.

the secondary, but depend of course directly on the assumed light ratio which is established by the photometry to an accuracy of at best 40 per cent. The derived colour correction is in agreement with that found from the depth of primary minimum ($0^m.63$ in B, $0^m.61$ in V, giving $-0^m.026$ as the differential colour index of the light lost from the primary, which corresponds to $-0^m.012$ in the $(b-y)$ index). Finally, we calculate the 'reddening-free' bracket indices defined as $[c_1] \equiv c_1 - 0.2(b-y)$, $[m_1] \equiv m_1 + 0.32(b-y)$, $[u-b] \equiv [c_1] + 2[m_1]$, and find

$$[c_1]^I = 0.972 \pm 10, [m_1]^I = 0.160 \pm 6, [u-b]^I = 1.292 \pm 16$$

for component 1 alone. These indices closely resemble a slightly reddened, apparently unevolved main-sequence star of spectral type A0 V: in fact, the MK calibration of Jakobsen (1985b) gives A0 V_{ext} ('ext' meaning that the star lies below the concentrated luminosity class V 'box' in the $[c_1]$-$[m_1]$-diagram; Fig. 6), and her empirical $T_{eff}([u-b])$ calibration (Jakobsen 1985a) indicates a temperature of 9900 K, while her revision of Strömgren's (1966) T_{eff}(a) calibration gives $10\,000\ \mathrm{K} + 2.33 \times 10^4\ [E(b-y) - 0.036]$, depending on the adopted colour excess (see below).

A useful comparison is also possible with theoretical Strömgren indices computed from the Kurucz (1979) model atmosphere grid and transformed to the standard system using secondary spectrophotometric standards for calibration (Lester *et al.* 1986). We determine from their solar composition grid by interpolation in the $[c_1]$-$[m_1]$-diagram (Fig. 4)

$$T_{eff} = 10\,080\ \mathrm{K} \pm 100; \log g = 4.224 \pm 0.050.$$

Consistency with the $[m_1]$-$(b-y)$-diagram then requires us to adopt $(b-y)_0 = -0.015$, hence $E(b-y) = 0.038$ (*cf.* Fig. 5). Let us mention that Hilditch, Hill & Barnes' (1983; HHB) empirical *uvbyβ* intrinsic colour calibration and dereddening algorithm for A intermediate stars yields instead $(b-y)_0 = 0.00$ at $m_0 = 0.160$, hence $E(b-y) = 0.023$; the observed c_1 index, however, is too small by 0.09 compared to their calibration. On the other hand, consideration of the c_1 versus $(b-y)$ diagram for the calibration stars (HHB's fig. 2) would lead us to adopt Crawford's (1978) late B-type star calibration instead, giving $(b-y)_0 = -0.024$ at $c_0 = 0.97$, hence $E(b-y) = 0.047$; in this case, however, the dereddened m_1 index is too large by 0.03 and V 836 Cyg falls below the calibration line in the m_1 versus $(b-y)$ diagram. We conclude that

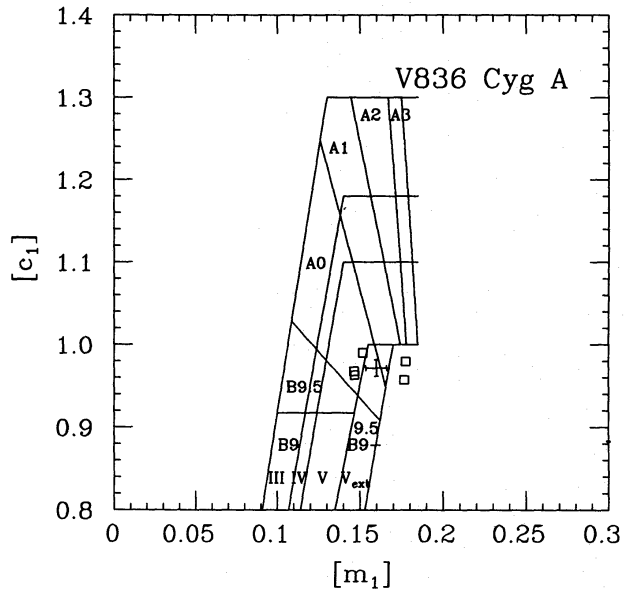

Figure 6. Same as Fig. 4, but now calibrated in terms of MK classes (adapted from Jakobsen 1985b, fig. 3).

neither calibration line fits the observed indices and that we have to adopt an $E(b-y)$ somewhere between to get overall consistency.

The result for log g locates the primary component not far from the ZAMS [the exact location of the boundary being independent on the chemical composition, see, e.g., Hejlesen 1980; for $Z=0.02$, his models give $\delta(\log g)=0.14$]. There is no quantitative measure of $[M/H]$ for component 1. The m_1-index, designed to determine metal abundances for cooler stars, requires high precision photometry and is, moreover, unsuited for early spectral classes ($T_e \geq 7500$ K), where it depends on T_e and g rather than on abundance effects. It suffices, however, to derive a crude estimate for $\delta m_0 \equiv m_0(\text{ZAMS}) - m_0(\text{observed})$, which falls in the range $-0.01 \leq \delta m_0 \leq 0.025$, and therefore classifies component 1 as a normal population I star (see e.g. Moon 1985).

The only information we have on the radiative properties of the secondary comes from the considerably uncertain and solution-dependent surface brightness ratios in the B and V bands (see above). For our reference model solution, we derived through comparison with the empirical flux scales of Popper (1980; Table 1) a temperature of log $T_e = 3.756$ and a colour difference $\Delta(B-V)=0.72$ from the flux ratio in V, and log $T_e = 3.767$, $\Delta(B-V)=0.67$ from the flux ratio in B, assuming log $T_e = 4.00$ for the primary. As we used the Wilson–Devinney code in mode 2 (temperatures and surface brightness ratio coupled via Planck's law), our simultaneous B and V solutions are bound to yield unrealistic 'blackbody' colour indices [in this case $\Delta(B-V)=0.54$ instead of 0.70], if these were evaluated directly from the obtained light ratios in B and V (because the errors add up then and may not compensate each other).

4 Absolute dimensions and evolutionary status

It is also possible, by combining the light curve solution ($i = 80\overset{\circ}{.}7 \pm 0\overset{\circ}{.}4$ for $0.30 \leq q \leq 0.5$; Fig. 2a) with the mass function, $f(\mathcal{M}) = 0.050 \pm 0.005$ (Duerbeck & Schumann 1982), to evaluate the individual masses, absolute dimensions, and thereby log g, as functions of the mass ratio (Fig. 2a and b). A plot of the resulting values against q for the photometric 'best fit' range $0.3 \leq q \leq 0.5$ shows that $\log g = 4.22 \pm 0.05$ is attained only for mass ratios around $q = 0.34 \pm 0.04$, thereby confining the mass ratio to a narrow interval towards the lower end of the photometric best fit range.

It has been shown by Hill *et al.* (1976) that, even at very low light, secondary blending with the broad Balmer wings of component 1 may lead to a non-negligible systematic underestimate of the primary amplitude variation, which in turn may reduce the value of $f(\mathcal{M})$ up to 10 per cent. However, even when varying the upwards corrected mass function within the limits $0.05 \leq f(\mathcal{M}) \leq 0.06$, the previous results are only slightly modified.

The resulting rough estimates for the absolute dimensions of components 1 and 2 given in Table 5 finally allow consideration of the evolutionary status of the binary system: the primary, being well detached from its Roche limiting surface, occupies, as a little-evolved A0 V star, a locus not far from the ZAMS boundary, while the G-type secondary marginally underfills its Roche lobe (Fig. 7) as a subgiant that is somewhat overluminous for its mass and temperature, but is still fairly close to the main sequence. For mass ratios near the lower end of the acceptable q range, the secondary gets in contact with its Roche lobe (Fig. 2b), and our data are not accurate enough to exclude such a truly semi-detached configuration. However, it is clear that, contrary to the conjecture made in Paper I, V 836 Cyg must be in a state following the phase of rapid mass exchange (case A); mass ratio reversal has occurred, the gainer has adjusted itself to remain as a more massive star on the main sequence, and the observed period increase ($\dot{P}/P \approx 1 \times 10^{-7}$ yr^{-1}, on the average, during 60 yr) might be explained as resulting from the slow outflow of mass from the now less-massive secondary on to the primary, proceeding

Table 5. Astrophysical data[1] for V 836 Cygni.

	Primary	Secondary
P (day)	0.6534	
q	0.34 ± 0.04	
H (10^{52} g cm^2 s^{-1})	1.4 ± 0.5	
h (10^{18} cm^2 s^{-1})	11.8 ± 2.5	
$\log[q(1+q)^{-2}P^{1/3}]$	−0.784 ± 0.025	
$\mathcal{M}/\mathcal{M}_\odot$	2.4 ± 0.8	0.80 ± 0.15
$\mathcal{R}/R_\odot$	1.96 ± 0.17	1.24 ± 0.11
ρ (g cm^{-3})	0.42 ± 0.02	0.57 ± 0.05
$\log g$ (cgs)	4.22 ± 0.05	4.15 ± 0.03
T_e (K)	10000 ± 200	$5770 \pm \frac{150}{500}$
$\log L/L_\odot$	1.54 ± 0.11	$0.18 \pm \frac{0.12}{0.24}$
M_{bol}	0.79 ± 0.25	$4.18 \pm \frac{0.6}{0.3}$
$B.C.$	−0.25	−0.14
M_{vis}	1.04 ± 0.25	$4.32 \pm \frac{0.65}{0.35}$
$E(b-y)$	0.038 ± 0.01	
V	8.68 ± 0.01	
Distance (pc)	320 ± 40	

[1] H = Orbital angular momentum; h = angular momentum per unit of reduced mass; $\log[q(1+q)^{-2}(\mathrm{P/d})^{1/3}] \approx H/\mathcal{M}^{5/3}$; ρ = mean densities; P = orbital period.

on a nuclear time-scale (for conservative transfer, a transfer rate of $\dot{\mathcal{M}} \approx 4 \times 10^{-8} \mathcal{M}_\odot$ yr^{-1} would be implied). Light-curve distortions may be related to instabilities around the inner Lagrangian point. Obviously, evolution in this system cannot have proceeded conservatively: if we assume conservation of total mass and orbital angular momentum in the binary system, and retrace its evolution back to the point where the present lobe-filling star was equal in mass ($1.6\mathcal{M}_\odot$) to its companion, we obtain a system of $0^d.28$ period, a semi-major axis of $2.7\mathcal{R}_\odot$, and a Roche lobe radius of $1.0\mathcal{R}_\odot$, far too small to fit the stars into the system. We conclude that V 836 Cygni must have lost a significant fraction (25 per cent or more) of its orbital angular momentum (and probably also some mass) during its evolution. Finally we should mention that chromospheric activity of the rapidly rotating G-type subgiant secondary in combination with mass loss through a convectively driven stellar wind mechanism may also play an important role for this close binary system (*cf.* Hall & Kreiner 1980).

V 836 Cyg joins the small group of short-period non-contact close binary systems showing EB-type light curves (*cf.* Yamasaki *et al.* 1988; Hilditch *et al.* 1988). Besides short-period detached and marginal contact systems this heterogeneous group comprises ordinary sd systems. Most of these consist of a main-sequence star of spectral type A–F and a Roche lobe filling (or nearly so) subgiant secondary of spectral type G–K. Unlike the classical Algols, the Roche lobe filling star is only moderately oversized and in most cases it is the smaller one. Also, the mass ratios encountered are less extreme (around $\frac{1}{3}$). Most of these are thought to be post mass-transfer remnants and the review by Hilditch *et al.* (1988) suggests an evolutionary path leading from longer period detached systems via case A mass transfer and angular momentum loss to semi-detached systems, further to marginal contact systems, and finally to the deeper contact A-type systems. In the evolution-sensitive mass–radius plane, the secondary

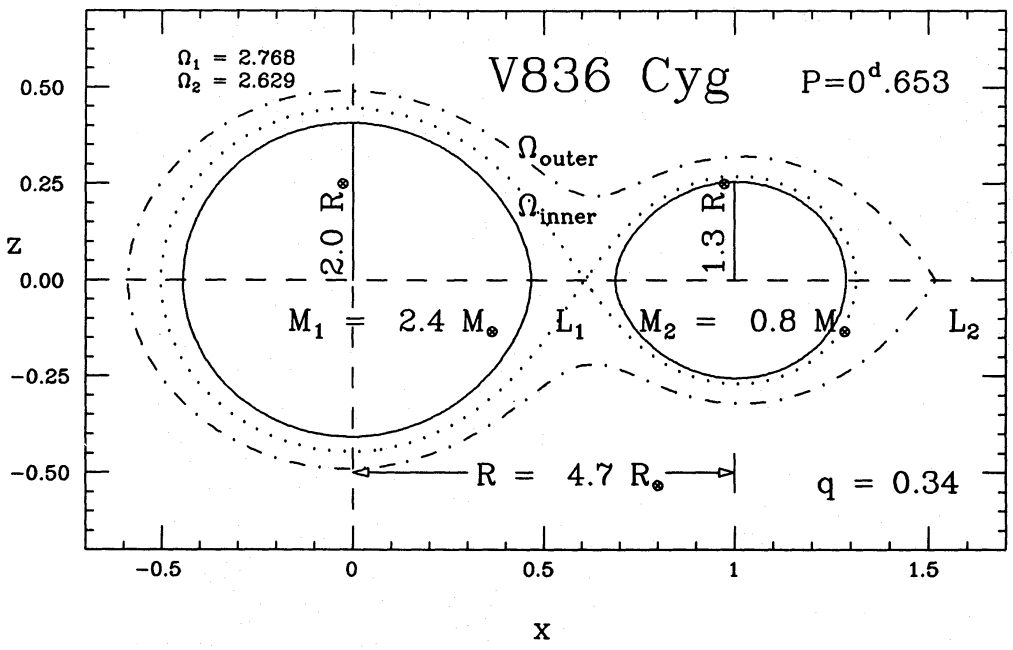

Figure 7. Geometric configuration of the system V 836 Cygni (axial cross-section).

of V 836 Cyg occupies a similar position as the secondaries of A-type W UMa systems. V 836 Cyg is a relatively early member of this group, on the boundary to the short-period early-type semi-detached systems now also believed to be examples of case A mass transfer (*cf.* Semeniuk & Kaluzny 1984; Hilditch & Bell 1987). A similar system that is, however, still in the rapid phase of mass transfer before mass ratio reversal, is V 388 Cyg ($P = 0.859$ d, A3 + G, *cf.* Milano & Russo 1983). *uvbyβ* as well as *RI* photometry and better spectroscopy are required to determine more accurately the properties of the secondaries and to elucidate the evolutionary status of these systems. Due to its rotationally broadened lines (at synchronous rotation $v_1 \sin i \cong 152$ km s^{-1}, $v_2 \sin i \cong 96$ km s^{-1}) and a magnitude difference of 4 mag in the blue spectral region, detection of the secondary spectrum of V 836 Cyg will, unfortunately, be extremely difficult, even with modern Reticon detectors applied in the longwave spectral region.

Acknowledgments

It is a great pleasure to thank Dr M. T. Karimie, who contributed to the reduction and analysis of the DB1 and DB2 data. JK gratefully acknowledges financial support from a stipendium of the Cusanuswerk Foundation (Federal Republic of Germany).

References

Böhm-Vitense, E., 1981. *Ann. Rev. Astr. Astrophys.*, **19**, 295.
Breinhorst, R. A. & Duerbeck, H. W., 1982. *J. Astrophys. Astr.*, **3**, 219.
Crawford, D. L., 1978. *Astr. J.*, **83**, 48.
Duerbeck, H. W. & Breinhorst, R. A., 1984. *Veröff. astr. Inst. Univ. Bonn*, No. 98.
Duerbeck, H. W. & Schumann, J. D., 1982. *J. Astrophys. Astr.*, **3**, 233.
Hall, D. S. & Kreiner, J. M., 1980. *Acta Astr.*, **30**, 387.
Harris, D. L., 1963. In: *Basic Astronomical Data*, p. 263, ed. Strand, K. Aa., University of Chicago Press, Chicago.
Hejlesen, P. M., 1980. *Astr. Astrophys. Suppl.*, **39**, 347.

Hilditch, R. W., 1981. *Mon. Not. R. astr. Soc.*, **196,** 305.
Hilditch, R. W. & Bell, S. A., 1987. *Mon. Not. R. astr. Soc.*, **229,** 529.
Hilditch, R. W. & Hill, G., 1975. *Mem. R. astr. Soc.*, **79,** 101.
Hilditch, R. W., Hill, G. & Barnes, J. V., 1983. *Mon. Not. R. astr. Soc.*, **204,** 241.
Hilditch, R. W., King, D. J. & McFarlane, T. M., 1988. *Mon. Not. R. astr. Soc.*, **231,** 341.
Hill, G., Hilditch, R. W., Younger, F. & Fisher, W. A., 1975. *Mem. R. astr. Soc.*, **79,** 131.
Hill, G., Aikman, G. C. L., Cowley, A. P., Bolton, C. T. & Thomas, J. C., 1976. *Astrophys. J.*, **208,** 152.
Hutchings, J. B. & Hill, G., 1971. *Astrophys. J.*, **166,** 373.
Jakobsen, A. M., 1985a. *Empirical Calibrations between Effective Temperatures, Bolometric Corrections and* uvby-β *Photometry for B- (A–F) Type Stars,* Preprint.
Jakobsen, A. M., 1985b. *Calibrations between* uvby-β *Photometry and MK-Classes,* Preprint.
Kallrath, J. & Linnell, A. P., 1987. *Astrophys. J.*, **313,** 346.
Kaluzny, J. & Semeniuk, I., 1984. *Acta Astr.*, **34,** 433.
Koch, R. H., 1973. *Astr. J.*, **78,** 410.
Kopal, Z., 1959. *Close Binary Systems,* Chapman & Hall, London.
Kurucz, R. L., 1979. *Astrophys. J. Suppl.*, **40,** 1.
Lester, J. B., Gray, R. O., Kurucz, R. L., 1986. *Astrophys. J. Suppl.*, **61,** 509.
Milano, L. & Russo, G., 1983. *Mon. Not. R. astr. Soc.*, **203,** 235.
Moon, T. T., 1985. *Communs Univ. London Obs.*, No. 78.
Popper, D. M., 1980. *Ann. Rev. Astr. Astrophys.*, **18,** 115.
Rafert, J. B. & Markworth, N. L., 1986. *Astr. J.*, **92,** 678.
Russell, H. N. & Merrill, J. E., 1952. *Contr. Princeton Univ. Obs.*, No. 26.
Semeniuk, I. & Kaluzny, J., 1984. *Acta Astr.*, **34,** 207.
Strömgren, B., 1966. *Ann. Rev. Astr. Astrophys.*, **4,** 433.
Wester, J., 1977. *Diploma thesis,* University of Tübingen.
Wilson, R. E. & Devinney, E. J., 1971. *Astrophys. J.*, **166,** 605.
Wood, D. B., 1971. *Astr. J.*, **76,** 701.
Yamasaki, A., Okazaki, A. & Kitamura, M., 1988. *Publs astr. Soc. Japan,* **40,** 79.

Appendix A: Imposing a constraint for the absolute radius of one component

In connection with the SIMPLEX algorithm as an optimization procedure for parameters derived from the Wilson–Devinney model (*cf.* Kallrath & Linnell 1987), it is possible to impose a constraint which forces a light-curve solution to reproduce the 'correct' radius of a main-sequence star. Let P denote the period of the binary, $\mathscr{R}_i$ the radius of component i, and $\mathscr{M}_j$ the mass of component j. If a Keplerian orbit is assumed for the binary, the mean distance $\mathscr{A}$ between both stars is given by

$$\mathscr{A}^3=(\mathscr{M}_1+\mathscr{M}_2)P^2, \tag{1}$$

in units of solar masses, astronomical units and years so that $G=4\pi^2$. If one of both masses is known, the other can be calculated for a specific mass ratio q according to

$$\mathscr{M}_2=q\mathscr{M}_1 \leftrightarrow \mathscr{M}_1=\frac{1}{q}\mathscr{M}_2. \tag{2}$$

For an arbitrary mass ratio q the quantities $\mathscr{R}_i$ and $\mathscr{M}_j$ define

$$r_i^\star := r_i^\star(q,\mathscr{R}_i,\mathscr{M}_j,P)=\mathscr{R}_i/\mathscr{A}(q,\mathscr{M}_j,P). \tag{3}$$

In equation (3) we may as well impose a mass–radius relation of the form $\mathscr{R}_i=\mathscr{R}(\mathscr{M}_i)$ and set $\mathscr{M}_i=\mathscr{M}(q,\mathscr{M}_j)$ or $\mathscr{M}_i=\mathscr{F}[q,f(\mathscr{M})]$ depending on whether we presume the mass of one component or the system's mass function. In any case $r_i^\star$ reduces to a function of q. The Wilson–Devinney model generates stellar surfaces based on q and Roche potential values Ω_i.

We calculate the volume V_i of these stars and define a mean radius

$$r_i := r_i(q, \Omega_i) = \left[\frac{3}{4\pi} V_i\right]^{1/3}. \tag{4}$$

Imposing $r_i^\star = r_i$ guarantees that the absolute radius of component i is $\mathscr{R}_i$, or, alternatively, that it obeys the mass–radius relation: $\mathscr{R}_i = \mathscr{R}(m_i)$. Thus we achieve an implicit equation for Ω_i:

$$r_i(q, \Omega_i) = r_i^\star(q). \tag{5}$$

Note that Ω_i is given in the frame of star 1. The value of Ω_2 in the frame of star 2 (denoted Ω_2') is given by

$$\Omega_2 = q\Omega_2' + \frac{1}{2}(1-q), \qquad q' := \frac{1}{q}. \tag{6}$$

An approximate relation between the mean r_i and Ω_i is given by Kopal (1959, p. 129) as

$$r \approx \frac{1}{\Omega - q}. \tag{7}$$

Equation (5) may be solved with the Newton–Raphson algorithm

$$\Omega^{(n+1)} = \Omega^{(n)} - \frac{r(\Omega^{(n)}, q) - r^\star(q)}{\dfrac{dr}{d\Omega}[\Omega^{(n)}, q]}, \tag{8}$$

where the subscripts have been neglected. The initial values for the iteration are derived from equation (7)

$$\Omega_1^{(0)} = \frac{1}{r_1} + q, \qquad \Omega_2^{(0)} = q\left[\frac{1}{r_2} + \frac{1}{q}\right] + \frac{1}{2}(1-q). \tag{9}$$

The derivatives $(dr/d\Omega)$ are approximated by differences

$$\frac{dr}{d\Omega} = \frac{r(\Omega + \Delta\Omega) - r(\Omega)}{\Delta\Omega}, \tag{10}$$

where $\Delta\Omega = 0.01$ is a good choice. The iteration is stopped when

$$|r(\Omega, q) - r^\star(q)| < \varepsilon = 0.001 \tag{11}$$

is fulfilled.